Published in final edited form as:
Prostate. 2008 July 1; 68(10): 1116–1125. doi:10.1002/pros.20776.

Zoledronic Acid Decreased Osteolysis But Not Bone Metastasis in a Nude Mouse Model of Canine Prostate Cancer With Mixed Bone Lesions

Nanda K. Thudi[1], **Chelsea K. Martin**[1], **Murali V.P. Nadella**[1], **Soledad A. Fernandez**[2], **Jillian L. Werbeck**[1], **Joseph J. Pinzone**[3], and **Thomas J. Rosol**[1,*]

[1]Department of Veterinary Biosciences, The Ohio State University, Columbus, Ohio

[2]Center for Biostatistics, The Ohio State University, Columbus, Ohio

[3]Department of Internal Medicine, The Ohio State University, Columbus, Ohio

Abstract

BACKGROUND—Bone metastasis is the most common cause of morbidity and mortality in patients with advanced prostate cancer and is manifested primarily as mixed osteoblastic and osteolytic lesions. However, the mechanisms responsible for bone metastases in prostate cancer are not clearly understood, in part due to the lack of relevant in vivo models that mimic the clinical presentation of the disease in humans. We previously established a nude mouse model with mixed bone metastases using intracardiac injection of canine prostate cancer cells (Ace-1). In this study, we hypothesized that tumor-induced osteolysis promoted the incidence of bone metastases and osteoblastic activity.

METHODS—We studied the effect of inhibition of osteolysis with zoledronic acid (ZA) on the prevention and progression of Ace-1 bone metastases in nude mice using prophylactic and delayed treatment protocols. Bioluminescent imaging, radiography, and histopathological evaluation were performed to monitor the effect of ZA on the incidence, progression and nature of bone metastases.

RESULTS—Unexpectedly, there was no significant difference in tumor burden and the incidence of metastasis between control and treatment groups as detected by bioluminescent imaging and bone histomorphometry. However, radiographic and histopathological analysis showed a significant treatment-related decrease in osteolysis, but no effect on tumor-induced trabecular bone thickness in both treatment groups compared to controls.

CONCLUSION—Our results demonstrated that the incidence of prostate cancer bone metastases in vivo was not reduced by zoledronic acid even though zoledronic acid inhibited bone resorption and bone loss associated with the mixed osteoblastic/osteolytic bone metastases in the Ace-1 model.

Keywords

prostate cancer; bioluminescent imaging; bone metastases; zoledronic acid; osteoblastic metastases; osteolysis

*Correspondence to: Dr. Thomas J. Rosol, Department of Veterinary Biosciences, College of Veterinary Medicine, The Ohio State University, 1925 Coffey Road, Columbus, OH 43210. rosol.1@osu.edu.

INTRODUCTION

Prostate cancer is the most frequently diagnosed cancer and second leading cause of cancer-related deaths in men [1]. In spite of themarked improvements in early diagnosis and efficient local and systemic therapeutic approaches, 65–75%of the patients with advanced prostate cancer develop skeletal metastasis due to the resistance of tumor cells to conventional therapies [2–4]. In prostate cancer, most patients die because of metastases to bone rather than the primary tumor [5].

Prostate cancer bone metastasis is frequently osteoblastic in nature with increased woven bone formation often preceded by osteoclastic activity [2,6]. Currently, in prostate cancer, the mechanisms responsible for osteoblastic bone metastases are not clear due to the lack of prostate cancer cell lines that consistently metastasize to bone and develop mixed osteoblastic and osteolytic lesions in animal models. Therefore, prostate cancer cell lines that reliably develop mixed osteoblastic and osteolytic lesions in vivo can be used to help understand the mechanisms underlying mixed bone metastases of prostate cancer as they occur in men. Recently, we have established a new canine prostate cancer cell line (Ace-1) from a prostate adenocarcinoma that consistently produces mixed osteoblastic and osteolytic bone metastases after intracardiac injection in nude mice [7,8]. Metastases of prostate cancer occur in the axial and appendicular bones in humans. Spontaneous prostate cancer in dogs has important similarities to human prostate cancer in the clinical presentation of disease including tumor growth over a long period of time, individual and intratumor heterogeneity, extensive genome homology, and metastasis to distant sites, such as bone. Metastasis of Ace-1 cells and development of mixed osteoblastic/osteoblastic lesions in nude mice recapitulates the characteristics of human and canine prostate cancer metastases in a mouse model [9,10]. Therefore, the Ace-1 model is useful to study the pathogenesis of prostate cancer metastasis and investigate the complex interactions between tumor cells and the bone microenvironment.

Preferential metastasis and growth of prostate cancer cells in bone is associated with a complex interactions between the cancer cells (seed), bone cells, and the bone marrow microenvironment (fertile soil) [3,11]. Metastatic prostate cancer cells in bone produce factors such as parathyroid hormone related protein (PTHrP) and receptor activator for nuclear factor κ B ligand (RANKL) that stimulate increased bone resorption [5]. This results in the further release of growth factors and proteins from the bone matrix that promote the growth of cancer cells in bone and possibly increase the maturation and function of osteoblasts. Therefore, it has been hypothesized that bone resorption contributes significantly to the development of osteoblastic metastases. However, the role of osteolysis in prostate cancer bone metastasis, growth of metastases, and induction of osteoblasts is not well understood [5,12–15]. Therefore, targeting osteoclast activity in mixed osteoblastic and osteolytic bone metastases will improve our understanding of the mechanisms underlying prostate cancer bone metastasis. Insights into the pathogenesis of prostate cancer bone metastasis will help identify specific targets for effective therapeutic approaches to help treat this devastating malignancy.

Previous studies have shown that zoledronic acid (ZA) is a potent inhibitor of osteoclastogenesis and osteoclast-mediated bone resorption in animal models of bone metastasis associated with prostate cancer, breast cancer and myeloma [16–20]. In the present study, we used ZA to inhibit osteoclast activity and investigate the role of osteoclast activity in prostate cancer bone metastasis.

MATERIALSANDMETHODS

Cell Culture

Ace-1 is a spontaneously immortalized canine prostate cancer cell line derived from a prostate adenocarcinoma that was previously established in our laboratory [7]. Ace-1 cells were maintained at 37°C in Dulbecco's Modified Eagle's Medium/Ham's Nutrient Mixture F12 (Invitrogen Corp., Carlsbad, CA) supplemented with 10% fetal bovine serum, 250 U/ml penicillin, 250 μg/ml streptomycin, and 2 mM L-glutamine (Invitrogen Corp.) in a 5% CO_2-humidified chamber.

Establishment of Ace-1 Cells Stably Expressing the YFP-Luc Reporter Gene

Ace-1 cells were transfected with 6 μg of pcDNA3.1(+)/YFP-LUC, a dual reporter gene construct under control of the CMV promoter (a generous gift from Dr. Christopher Contag, Stanford University, Stanford, CA), and 10 μl of Lipofectamine 2000 (Invitrogen Corp.). Stably integrated cells were selected using 400 μg/ml of G418 (Sigma–Aldrich Co., St. Louis, MO) for 17 days. Flow cytometry (BDFACSVantage SE; BD Biosciences, San Jose, CA) was used to sort and clone YFP-positive cells.

Intracardiac Inoculation of Ace-1 Cells Into Nude Mice

Male nu/nu mice, 4–6 weeks old (Charles River Laboratories, Wilmington, MA) were housed in microisolator cages, and were provided food pellets and water ad libitum. Animal care procedures were approved by the Ohio State University Institutional Lab Animal Care and Use Committee using criteria based on both the Animal Welfare Act and the Public Health Services "Guide for the Care and Use of Laboratory Animals." Mice were anesthetized with ketamine (100 mg/kg) and xylazine (10 mg/kg) administered intraperitoneally (IP) and positioned on dorsal recumbency. 1×10^5 Ace-1 cells were suspended in 100 μl of sterile Dulbecco's PBS (Invitrogen Co.) and were injected into the left ventricle using a 27 gauge needle after confirmation of location of the tip of the needle in the left ventricle indicated by pulsatile blood flow in the hub of the needle [21]. Successful Ace-1 intracardiac injections were confirmed using bioluminescent imaging (BLI) at 10 min after injection and were characterized by a diffuse emission of light from the entire body. Mice were euthanized 28 days after Ace-1 inoculation.

Treatment

Nude mice were divided into three groups: (a) Control group(n = 11) received PBS from –1 to 4weeks. (b) Prophylaxis group (n = 9) received ZA from –1 to 4 weeks. (c) Delayed treatment (n = 7) group received ZA from 2 to 4 weeks. Mice were administered ZA at 100 μg/kg BW (Novartis, Basel, Switzerland) or vehicle (PBS) twice a week subcutaneously (SQ) (Fig. 1).

Bioluminescent Imaging (BLI)

Mice were injected intraperitoneally (IP) with 150 μl 40 mg/ml luciferin (Caliper Life Sciences, Hopkinton, MA) dissolved in PBS. Mice were anesthetized with 3% isoflurane–air mixture and transferred to the light-tight 37°C imaging chamber of an In Vivo Imaging System (IVIS; Caliper Life Sciences). BLI was performed 10 min after IP administration of luciferin. BLI was performed on mice with dorso-ventral positioning under anesthesia with 1.5% isoflurane–air mixture once per week for 4 weeks. The BLI signal intensity was analyzed using LivingImage software version 2.50 (Caliper Life Sciences) and was quantified serially by measurement of peak photon flux at the individual metastasis foci by selecting a region of interest (ROI) around the BLI signal.

Faxitron Radiography

Radiographic images of mice were obtained using a Faxitron cabinet X-ray system (Hewlett-Packard, McMinnville, OR) at 45 kVp for 3.5 min at day 28.

Histopathology

Complete necropsies were performed on the mice. Bones were fixed in 10% neutral-buffered formalin at 4°C for 24 hr, decalcified in 10% EDTA (pH 7.4) for 2 weeks at 4°C, and embedded in paraffin. The specimens were sectioned (5 μm) and were stained with hematoxylin and eosin (H&E) to evaluate by histopathology or stained for tartrate-resistant acid phosphatase (TRAP) to identify active osteoclasts. TRAP staining was performed on non-stained sections that were deparaffinized by three 1 min washes with xylene (Hemo-De, Fisher Scientific, and Bay Shore, NY) and rehydrated in decreasing concentrations of ethanol (100%, 95% and finally 70%). For the effective staining of TRAP, antigen retrieval on the sections was performed using heat treatment at 60°C for 10 min in preheated antigen retrieval solution (Dako-Cytomation, Carpinteria, CA) and then stained for TRAP (Acid Phosphatase Kit 387-A; Sigma Diagnostics, St. Louis, MO) as directed by the manufacturer.

Bone Histomorphometry

Bone histomorphometry was performed using computer software designed for histomorphometric analyses (Image Pro plus version 5.0; Media Cybernetics, Silver Spring, MD). The number of large active osteoclasts (TRAP-positive osteoclasts with three or more nuclei) per millimeter of trabecular bone were measured along the tumor-bone interface in five different fields at 200× magnification for each bone. Trabecular volume in the metaphyses of long bones was measured in five different fields at 200× magnification for each bone. Total tumor area in the medullary cavity of each bone was measured at 400× magnification. The terminology used to describe bone histomorphometric parameters was recommended by the Histomorphometry Nomenclature Committee of the American Society for Bone and Mineral Research [22].

Serum Dickkopf-1 Enzyme-Linked Immunosorbent Assay (ELISA)

Serum Dkk1 levels were measured using the DuoSet Human Dkk1 ELISA Kit, as recommended by the manufacturer (R&D Systems, Minneapolis, MN). The lowest standard of the assay was 62.5 pg/ml.

Serum Osteocalcin Assay

Serum mouse osteocalcin levels were measured using an immunoradiometric assay according to the manufacturer's protocol (American Laboratory Products Company, Salem, NH). The polyclonal goat antibody used in this assay detects the mid-region and C-terminal portion of osteocalcin. The sensitivity of the assay was 0.1 ng/ml.

Statistics

Results were displayed as means ± standard error of mean (SEM). Data were analyzed using Student's *t*-test and multiple group comparisons were made by one-way ANOVA and Kruskal–Wallis test followed by Dunn's post hoc test. Data with P values less than 0.05 were considered statistically significant. ANOVA models were used for the comparisons of serum Dkk1 levels (Fig. 6C) and serum osteocalcin (Fig. 6A), and Dunnett's method was used to adjust for multiple comparisons between control or vehicle groups. One observation from the "delayed" group was removed because statistical diagnostics indicated that it was highly influential and resulted in bad fits. For the outcome variable serum osteocalcin, the Bonferroni correction

method was used to adjust for multiplicity for the six pairwise comparisons of interest. The statistical software SAS v.9 (Institute Inc., Cary, NC) was used for all the analyses.

RESULTS

Serial In Vivo Bioluminescent Imaging (BLI) of Ace-1 Tumor Growth and Metastasis Incidence in Nude Mice

To visualize and measure the effect of osteolysis on real-time tumor growth and incidence of metastasis in bone, Ace-1 prostate cancer cells stably expressing YFP-Luc reporter gene were injected into the left cardiac ventricle of nude mice. BLI of mice 10 min after intracardiac injection of Ace-1 cells revealed a bioluminescent signal over their entire bodies, which confirmed successful intracardiac injection of cancer cells. It was apparent from the signal intensity that tumor cells initially accumulated in the lungs, kidney, and brain immediately after intracardiac injection on day 0. However, metastases did not develop in these organs (Fig. 2A). At day 7, the diffuse BLI signal over the entire body was gone. By day 14, bone metastases in control, prophylactic and delayed treatment groups were identifiable in the vertebrae, humeri, tibias and femurs. There was no change in the number of metastatic foci during the course of the experiment, but there was increased intensity of bioluminescence signals at days 21 and 28 demonstrating progressive tumor growth in the bones. All mice in control, prophylactic and delayed treatment groups developed bone metastases over a period of 4 weeks after intracardiac injection of Ace-1 cells. Zoledronic acid (ZA) treatment had no significant effect on the BLI of tumor growth and incidence rate of metastases in prophylactic and delayed treatment groups compared to control mice (Fig. 2B,C). The BLI signals correlated well with the metastases in bones as demonstrated by radiography and histopathology (see below).

Faxitron Radiography

To characterize the Ace-1 bone metastases and confirm the metastatic sites observed by BLI, radiographs of all mice were taken on the day of sacrifice (day 28 after intracardiac inoculation of tumor cells) and representative radiographs are illustrated in Figure 3. In the tumor-bearing vehicle treatment group, the bone metastases had evidence of osteolysis characterized by loss of cortical and medullary bone in the metaphyses of long bones compared to intact cortical bone and radio-opaque medullary bone in the nontumor-bearing vehicle treatment group. In the delayed treatment group, intact cortical bone with mild osteolysis in the medullary region of the metaphysis was observed demonstrating inhibition of osteolysis by ZA. In the prophylactic treatment group, intact cortical bone with increased radio-opacity in the metaphyseal regions of the long bones demonstrated inhibition of osteolysis and the osteoblastic nature of the Ace-1 tumors following inhibition of osteolysis by ZA.

Histopathology

Based on BLI and radiography, we selected 13, 12, and 7 long bones from the control, prophylactic and delayed treatment groups, respectively, and stained sections from the bones with H&E. In the control group, the prostate carcinoma cells induced woven bone formation in the metaphyses adjacent to the neoplastic cells demonstrating their osteoblastic phenotype (Fig. 4A). There were multiple areas of cortical and trabecular bone resorption caused by tumor-induced increased osteoclast activity along the cortical and trabecular endosteum. In some of the bones there was reactive new bone formation in the periosteum adjacent to the tumor. In ZA-treated mice, Ace-1 metastases extended from the growth plate to the diaphysis and filled the marrow cavities in between metaphyseal trabeculae (Fig. 4A,B). To determine the effect of ZA on tumor-induced bone formation, we measured metaphyseal trabecular thickness adjacent to intramedullary metastases. Trabecular thickness adjacent to metastases was significantly ($P < 0.001$) increased in all tumor-bearing mice compared to contralateral bones in non-tumor bearing mice. ZA had no effect on tumor-induced trabecular thickness in

treatment groups compared to the control group (Fig. 4C). Histomorphometry demonstrated that ZA had no significant effect on the tumor area in bone metastases (Fig. 4D).

TRAP staining was performed on the bone sections to identify the active osteoclasts. Numerous TRAP-positive osteoclasts (with three or more nuclei) were observed along the tumor-bone interface in vehicle-treated mice compared to few active osteoclasts in the mice treated with ZA (Fig. 5A). Bone histomorphometry was performed on the TRAP-stained bone sections to quantify the effect of ZA on the osteoclast activity at the tumor-bone interface. ZA decreased TRAP-positive osteoclasts by five- to sixfold in tumor-bearing mice, as compared to vehicle-treated tumor-bearing mice (Fig. 5B).

Bone Remodeling Indices

Our results showed that ZA inhibited the prostate cancer-induced osteolysis, To determine and compare the effect of ZA on bone remodeling in healthy mice and in tumor-bearing mice, we measured serum osteocalcin following treatment of mice for 4 weeks. ZA treatment significantly ($P < 0.0001$) decreased serum osteocalcin concentrations in nontumor-bearing mice. In contrast, ZA treatment did not reduce serum osteocalcin in tumor-bearing mice (Fig. 6A). Bone histomorphometric analysis showed that ZA treatment of healthy mice for 4 weeks increased the trabecular volume by twofold (Fig. 6B) compared to the vehicle-treated mice. The decreased serum osteocalcin and increased trabecular bone volume in ZA-treated healthy mice demonstrated the effect of ZA on the inhibition of normal physiological bone remodeling.

It has been shown that Dkk1 promotes osteolysis and inhibits osteoblast differentiation by antagonizing the Wnt signaling pathway in prostate cancer bone metastases [23,24]. To determine the role of Dkk1 in this study, we measured serum Dkk1 concentrations. Dkk1 concentrations in tumor-bearing mice (avg = 4.2 ng/ml) were significantly increased compared to nontumor-bearing mice (avg = 1.9 ng/ml). ZA significantly decreased Dkk1 concentrations in the prophylactic treatment group but had no effect in delayed treatment mice as compared to vehicle-treated mice (Fig. 6C). This could be due to the long duration of ZA treatment in the prophylactic treatment compared to the delayed treatment. These data suggest that ZA-mediated inhibition of Dkk1 might contribute to the decreased osteolysis.

DISCUSSION

Prostate cancer metastases to bone are typically characterized by a predominance of new woven bone formation with a lesser amount of osteolysis (‘osteoblastic’ metastases) [23]. The contribution of osteolysis in the development of osteoblastic lesions in prostate cancer bone metastases is not well understood partially due to a lack of preclinical models that consistently develop mixed osteoblastic and osteolytic lesions [24–26]. This study showed that bone metastasis and osteoblastic lesions are independent of osteolysis in a nude mouse model of canine prostate cancer-induced mixed bone metastases.

Studies have shown that normal bone homeostasis is maintained by the balanced coupling of bone resorption and bone formation [27]. However, the importance of the bone remodeling sequence in the development of prostate cancer bone metastasis is unknown. Metastasis of prostate cancer cells to bone disrupts the balanced coupling of bone remodeling. Although bone formation and bone resorption are both increased, bone formation is favored and the remodeling process becomes unbalanced, resulting in a net gain of bone. Many studies have reported that both osteoclast and osteoblast activity are important for prostate cancer bone metastases [13]. Previously, the lack of preclinical models that recapitulate the sequential course of mixed bone metastases has prevented investigations on the in vivo significance of osteoclast activity in the development of osteoblastic lesions [23,28–31]. We have developed a canine prostate cancer cell line (Ace-1) that develops mixed bone metastases in nude mice

[7,8]. This model allows studies on the sequential biological events involved in the development of prostate cancer bone metastases.

To investigate the role of osteoclastic bone resorption in the development of osteoblastic metastases, we inhibited osteoclastic-mediated bone resorption in Ace-1 tumor-bearing mice using zoledronic acid (ZA). As expected, radiographic and histopathological findings showed that ZA markedly inhibited osteolysis of cortical and trabecular bone when compared to the control group, regardless of the administration schedule. Decreased number of TRAP-stained osteoclasts and decreased serum Dkk1 levels in the ZA-treated groups additionally supported this observation. Dkk1 was shown to decrease osteoblast maturation and mineralization in vitro and has the potential to switch the phenotype of bone metastasis from osteoblastic to osteolytic [32]. In the bone microenvironment, bone marrow mesenchymal stem cells (BMMSC) are the source of Dkk1 [33]. The exact mechanism of ZA inhibition on Dkk1 is not clear. Based on the findings in this study that ZA had no effect on the incidence of prostate cancer metastasis to bone or growth of bone metastases, but had decreased Dkk1 levels, we speculate that prostate cancer metastasis to bone stimulated Dkk1 expression in BMMSC. ZA inhibited the tumor-mediated stimulation of Dkk1 expression by BMMSC. Decreased Dkk1 levels might be one of the potential factors contributing be the decrease in osteolysis and increased bone formation in this model. The ability of ZA to inhibit osteolysis in our study was consistent with previous reports [16–18]. ZA was less effective in the delayed treatment group compared to the prophylactic group, suggesting that preventive therapy may be more effective to treat patients with osteolytic metastases in bone. On the other hand, the increased efficacy of prophylactic treatment in this study might be attributed to the longer duration of treatment (5 weeks) compared to shorter (2 weeks) administration in the delayed treatment group.

Recent studies have documented the ability of in vivo bioluminescent imaging (BLI) to measure tumor progression and response to therapy in animal models [34]. The BLI data revealed that ZA treatment had no significant effect on the incidence of bone metastases or the rate of metastatic tumor growth. Furthermore, analysis of tumor area using histomorphometry revealed no significant difference between treatment and control groups despite the significant inhibition of osteolysis. Our data is in agreement with the report from Saad et al. [35] that showed ZA had no effect on tumor progression and survival rate of prostate cancer patients. Lee et al. [16] showed that ZA was effective in inhibiting bone resorption induced by the prostate cancer cell line (PC-3); however, there was no effect on osteoblastic lesions induced by the LAPC-9 prostate cancer cell line. In contrast, Corey et al. [17] demonstrated that ZA inhibited tumor progression and osteoblastic lesions in an experimental mouse model with LuCaP 23.1 prostate cancer cells. These findings suggest the ability of ZA to inhibit tumor progression and osteoblastic metastasis depends on the specific biology of the prostate cancer cell line evaluated. Variation in the nature of different cell lines can be attributed to the heterogeneity of the primary prostate cancer from which cell lines are derived. Our findings demonstrate that the osteoclastic component of Ace-1- induced bone metastases were not necessary for the survival and growth of tumor in bone or development of osteoblastic metastases.

Osteocalcin, which is secreted by osteoblasts, is a bone turnover marker because the osteoblast-secreted osteocalcin is deposited in bone matrix and released during bone resorption [36,37]. ZA significantly reduced serum osteocalcin in nude mice, indicating a reduction in bone turnover. This finding was consistent with previously published work showing that ZA reduced osteocalcin concentrations in patients with prostate cancer bone metastases [38,39]. There was no significant difference in serum osteocalcin levels in Ace-1-bearing control mice compared to control nontumor-bearing mice. Koizumi et al. previously showed that serum osteocalcin concentrations were similar in human patients with and without prostate cancer bone metastases [28,40]. This correlated with our findings and suggested that osteocalcin is not a

useful marker to identify bone metastases. Serum bone specific alkaline phosphatase, secreted by osteoblasts, is a specific and reliable bone formation marker [41]. We were unable to measure the bone specific alkaline phosphatase concentrations in the mice due to the lack of assays that detect this marker in mice.

Many studies have reported that osteoclast and osteoblast regulatory factors expressed by prostate cancer cells can alter bone homeostasis either directly or indirectly. Prostate (PC-3) and breast (MDA-231) cancer cell lines that induce osteolytic bone metastases express cytokines that include RANKL, interleukin-1 (IL-1), tumor necrosis factor-a (TNF-α), PTHrP and cathepsin K, which are associated with increased osteoclastogenesis. In contrast, C4-2B and LAPC-9 cells (prostate cancer) and ZR-75-1 and MCF-7 cells (breast cancer), which induce osteoblastic metastases, express abundant osteoprotegerin (OPG), bone morphogenic protein-2 (BMP-2), BMP-4, BMP-6, vascular endothelial growth factor (VEGF), endothelin-1 (ET-1), platelet derived growth factor-BB (PDGF-BB), insulin growth factor-1 (IGF-1) and fibroblast growth factor-2 (FGF-2), which are known to stimulate osteoblast activity [16,24,42–45]. Yin et al. [46] showed that ET-1 production in ZR-75-1 cells stimulated osteoblast activity resulting in increased new bone formation. PDGF-BB, VEGF and urokinase plasminogen activator (uPA) also contributed to the increased bone formation in prostate and breast cancer bone metastases [24,47,48]. PCR analysis revealed that Ace-1 cells express a wide variety of factors known to stimulate both osteoclasts (RANKL, IL-6, cathepsin K, PTHrP) and osteoblast activity (PDGF-BB, ET-1, VEGF, uPA, OPG, FGF-2 and IGF-1) (unpublished data). The cytokine expression profile of Ace-1 cells suggests that multiple factors contribute to the osteoblastic and osteolytic phenotypes at metastatic sites. However, further investigations will be required to understand the role various cytokines in the development of mixed bone metastases in this model. In this regard, the Ace-1 model will be a very useful translational model to study the pathogenesis and treatment of prostate cancer bone metastasis.

Acknowledgments

We would like to thank Fu-Sheng Chou for his assistance with the ELISA assay and Tim Vojt for illustrations. This work was supported by the National Cancer Institute (CA100730 and CA77911) and the National Center for Research Resources (RR00168).

Grant sponsor: National Cancer Institute; Grant numbers: CA100730, CA77911; Grant sponsor: National Center for Research Resources; Grant number: RR00168.

REFERENCES

1. Jemal A, Siegel R, Ward E, Murray T, Xu J, Smigal C, Thun MJ. Cancer statistics 2006. CA Cancer J Clin 2006;56(2):106–130. [PubMed: 16514137]
2. Adami S. Bisphosphonates in prostate carcinoma. Cancer 1997;80(8 Suppl):1674–1679. [PubMed: 9362435]
3. Fidler IJ. The pathogenesis of cancer metastasis: The 'seed and soil' hypothesis revisited. Nat Rev Cancer 2003;3(6):453–458. [PubMed: 12778135]
4. Crawford ED. Skeletal complications in men with prostate cancer: Effects on quality-of-life outcomes throughout the continuum of care. Eur Urol Suppl 2004;3(5):10–15.
5. Mundy GR. Metastasis to bone: Causes, consequences and therapeutic opportunities. Nat Rev Cancer 2002;2(8):584–593. [PubMed: 12154351]
6. Charhon SA, Chapuy MC, Delvin EE, Valentin-Opran A, Edouard CM, Meunier PJ. Histomorphometric analysis of sclerotic bone metastases from prostatic carcinoma special reference to osteomalacia. Cancer 1983;51(5):918–924. [PubMed: 6681595]
7. Leroy BE, Thudi NK, Nadella MV, Toribio RE, Tannehill-Gregg SH, van Bokhoven A, Davis D, Corn S, Rosol TJ. New bone formation and osteolysis by a metastatic, highly invasive canine prostate carcinoma xenograft. Prostate 2006;66(11):1213–1222. [PubMed: 16683269]

8. Halvorson KG, Kubota K, Sevcik MA, Lindsay TH, Sotillo JE, Ghilardi JR, Rosol TJ, Boustany L, Shelton DL, Mantyh PW. A blocking antibody to nerve growth factor attenuates skeletal pain induced by prostate tumor cells growing in bone. Cancer Res 2005;65(20):9426–9435. [PubMed: 16230406]
9. Khanna C, Lindblad-Toh K, Vail D, London C, Bergman P, Barber L, Breen M, Kitchell B, McNeil E, Modiano JF, Niemi S, Comstock KE, Ostrander E, Westmoreland S, Withrow S. The dog as a cancer model. Nat Biotechnol 2006;24(9):1065–1066. [PubMed: 16964204]
10. Waters DJ, Hayden DW, Bell FW, Klausner JS, Qian J, Bostwick DG. Prostatic intraepithelial neoplasia in dogs with spontaneous prostate cancer. Prostate 1997;30(2):92–97. [PubMed: 9051147]
11. Hart IR, Fidler IJ. Role of organ selectivity in the determination of metastatic patterns of B16 melanoma. Cancer Res 1980;40(7):2281–2287. [PubMed: 7388794]
12. Clines GA, Guise TA. Hypercalcaemia of malignancy and basic research on mechanisms responsible for osteolytic and osteoblastic metastasis to bone. Endocr Relat Cancer 2005;12(3):549–583. [PubMed: 16172192]
13. Keller ET. Overview of metastasis and metastases. J Musculoskelet Neuronal Interact 2002;2(6):567–569. [PubMed: 15758397]
14. Yoneda T, Michigami T, Yi B, Williams PJ, Niewolna M, Hiraga T. Actions of bisphosphonate on bone metastasis in animal models of breast carcinoma. Cancer 2000;88(12 Suppl):2979–2988. [PubMed: 10898341]
15. Goltzman D. Mechanisms of the development of osteoblastic metastases. Cancer 1997;80(8 Suppl): 1581–1587. [PubMed: 9362425]
16. Lee YP, Schwarz EM, Davies M, Jo M, Gates J, Zhang X, Wu J, Lieberman JR. Use of zoledronate to treat osteoblastic versus osteolytic lesions in a severe-combined-immunodeficient mouse model. Cancer Res 2002;62(19):5564–5570. [PubMed: 12359769]
17. Corey E, Brown LG, Quinn JE, Poot M, Roudier MP, Higano CS, Vessella RL. Zoledronic acid exhibits inhibitory effects on osteoblastic and osteolytic metastases of prostate cancer. Clin Cancer Res 2003;9(1):295–306. [PubMed: 12538482]
18. Croucher PI, De Hendrik R, Perry MJ, Hijzen A, Shipman CM, Lippitt J, Green J, Van Marck E, Van Camp B, Vanderkerken K. Zoledronic acid treatment of 5T2MM-bearing mice inhibits the development of myeloma bone disease: Evidence for decreased osteolysis, tumor burden and angiogenesis, and increased survival. J Bone Miner Res 2003;18(3):482–492. [PubMed: 12619933]
19. Lipton A, Small E, Saad F, Gleason D, Gordon D, Smith M, Rosen L, Kowalski MO, Reitsma D, Seaman J. The new bisphosphonate, zometa (zoledronic acid), decreases skeletal complications in both osteolytic and osteoblastic lesions: A comparison to pamidronate. Cancer Invest 2002;20:45–54. [PubMed: 12442349]
20. Saad F, Schulman CC. Role of bisphosphonates in prostate cancer. Urology 2004;45:26–34.
21. Guise TA, Yin JJ, Taylor SD, Kumagai Y, Dallas M, Boyce BF, Yoneda T, Mundy GR. Evidence for a causal role of parathyroid hormone-related protein in the pathogenesis of human breast cancer-mediated osteolysis. J Clin Invest 1996;98(7):1544–1549. [PubMed: 8833902]
22. Parfitt AM, Drezner MK, Glorieux FH, Kanis JA, Malluche H, Meunier PJ, Ott SM, Recker RR. Bone histomorphometry: Standardization of nomenclature, symbols, and units. Report of the ASBMR histomorphometry nomenclature committee. J Bone Miner Res 1987;2(6):595–610. [PubMed: 3455637]
23. Percival RC, Urwin GH, Harris S, Yates AJ, Williams JL, Beneton M, Kanis JA. Biochemical and histological evidence that carcinoma of the prostate is associated with increased bone resorption. Eur J Surg Oncol 1987;13(1):41–49. [PubMed: 3102281]
24. Kitagawa Y, Dai J, Zhang J, Keller JM, Nor J, Yao Z, Keller ET. Vascular endothelial growth factor contributes to prostate cancer-mediated osteoblastic activity. Cancer Res 2005;65(23):10921–10929. [PubMed: 16322239]
25. Mundy GR. Endothelin-1 and osteoblastic metastasis. Proc Natl Acad Sci USA 2003;100(19):10588–10589. [PubMed: 12963808]
26. Roodman GD. Mechanisms of bone metastasis. N Engl J Med 2004;350(16):1655–1664. [PubMed: 15084698]
27. Rodan GA. Bone homeostasis. Proc Natl Acad Sci USA 1998;95:13361–13362. [PubMed: 9811806]

28. Koizumi M, Maeda H, Yoshimura K, Yamauchi T, Kawai T, Ogata E. Dissociation of bone formation markers in bone metastasis of prostate cancer. Br J Cancer 1997;75(11):1601–1604. [PubMed: 9184174]
29. Yoshida K, Sumi S, Arai K, Koga F, Umeda H, Hosoya Y, Honda M, Yano M, Moriguchi H, Kitahara S. Serum concentration of type I collagen metabolites as a quantitative marker of bone metastases in patients with prostate carcinoma. Cancer 1997;80(9):1760–1767. [PubMed: 9351545]
30. Garnero P, Buchs N, Zekri J, Rizzoli R, Coleman RE, Delmas PD. Markers of bone turnover for the management of patients with bone metastases from prostate cancer. Br J Cancer 2000;82(4):858–864. [PubMed: 10732759]
31. Koga H, Naito S, Koto S, Sakamoto N, Nakashima M, Yamasaki T, Noma H, Kumazawa J. Use of bone turnover marker, pyridinoline cross-linked carboxyterminal telopeptide of type I collagen (ICTP), in the assessment and monitoring of bone metastasis in prostate cancer. Prostate 1999;39(1):1–7. [PubMed: 10221259]
32. Hall CL, Bafico A, Dai J, Aaronson SA, Keller ET. Prostate cancer cells promote osteoblastic bone metastases through Wnts. Cancer Res 2005;65(17):7554–7560. [PubMed: 16140917]
33. Corre J, Mahtouk K, Attal M, Gadelorge M, Huynh A, Fleury-Cappellesso S, Danho C, Laharrague P, Klein B, Rème T, Bourin P. Bone marrow mesenchymal stem cells are abnormal in multiple myeloma. Leukemia 2007;21(5):1079–1088. [PubMed: 17344918]
34. Rehemtulla A, Stegman LD, Cardozo SJ, Gupta S, Hall DE, Contag CH, Ross BD. Rapid and quantitative assessment of cancer treatment response using in vivo bioluminescence imaging. Neoplasia 2000;2(6):491–495. [PubMed: 11228541]
35. Saad F, Gleason D, Murray R, Tchekmedyian S, Venner P, Lacombe L, Chin JL, Vinholes JJ, Goas JA, Chen B. Zoledronic Acid Prostate Cancer Study Group. Zoledronic acid prostate cancer study group. A. randomized, placebo-controlled trial of zoledronic acid in patients with hormone-refractory metastatic prostate carcinoma. J Natl Cancer Inst 2002;94(19):1458–1468. [PubMed: 12359855]
36. Ivaska KK, Hentunen TA, Vaaraniemi J, Ylipahkala H, Pettersson K, Vaananen HK. Release of intact and fragmented osteocalcin molecules from bone matrix during bone resorption in vitro. J Biol Chem 2004;279(18):18361–18369. [PubMed: 14970229]
37. Watts NB. Clinical utility of biochemical markers of bone remodeling. Clin Chem 1999;45(8 Pt 2):1359–1368. [PubMed: 10430819]
38. Schneider A, Kalikin LM, Mattos AC, Keller ET, Allen MJ, Pienta KJ, McCauley LK. Bone turnover mediates preferential localization of prostate cancer in the skeleton. Endocrinology 2005;146(4):1727–1736. [PubMed: 15637291]
39. Reid IR, Brown JP, Burckhardt P, Horowitz Z, Richardson P, Trechsel U, Widmer A, Devogelaer JP, Kaufman JM, Jaeger P, Body JJ, Brandi ML, Broell J, Di Micco R, Genazzani AR, Felsenberg D, Happ J, Hooper MJ, Ittner J, Leb G, Mallmin H, Murray T, Ortolani S, Rubinacci A, Saaf M, Samsioe G, Verbruggen L, Meunier PJ. Intravenous zoledronic acid in postmenopausal women with low bone mineral density. NEngl J Med 2002;346(9):653–661.
40. Plebani M, Bernardi D, Zaninotto M, De Paoli M, Secchiero S, Sciacovelli L. New and traditional serum markers of bone metabolism in the detection of skeletal metastases. Clin Biochem 1996;29(1):67–72. [PubMed: 8929827]
41. Gomez B Jr, Ardakani S, Ju J, Jenkins D, Cerelli MJ, Daniloff GY, Kung VT. Monoclonal antibody assay for measuring bone-specific alkaline phosphatase activity in serum. Clin Chem 1995;41(11):1560–1566. [PubMed: 7586543]
42. Lee Y. Differences in the cytokine profiles associated with prostate cancer cell induced osteoblastic and osteolytic lesions in bone. J Orthop Res 2003;21(1):62–72. [PubMed: 12507581]
43. Dai J, Keller J, Zhang J, Lu Y, Yao Z, Keller ET. Bone morphogenetic protein-6 promotes osteoblastic prostate cancer bone metastases through a dual mechanism. Cancer Res 2005;65(18):8274–8285. [PubMed: 16166304]
44. Uehara H, Kim SJ, Karashima T, Shepherd DL, Fan D, Tsan R, Killion JJ, Logothetis C, Mathew P, Fidler IJ. Effects of blocking platelet-derived growth factor-receptor signaling in a mouse model of experimental prostate cancer bone metastases. J Natl Cancer Inst 2003;95(6):458–470. [PubMed: 12644539]

45. Guise TA, Yin JJ, Mohammad KS. Role of endothelin-1 in osteoblastic bone metastases. Cancer 2003;97(3 Suppl):779–784. [PubMed: 12548575]

46. Yin JJ, Mohammad KS, Kakonen SM, Harris S, Wu-Wong JR, Wessale JL, Padley RJ, Garrett IR, Chirgwin JM, Guise TA. A causal role for endothelin-1 in the pathogenesis of osteoblastic bone metastases. Proc Natl Acad Sci USA 2003;100(19):10954–10959. [PubMed: 12941866]

47. Yi B, Williams PJ, Niewolna M, Wang Y, Yoneda T. Tumor-derived platelet-derived growth factor-BB plays a critical role in osteosclerotic bone metastasis in an animal model of human breast cancer. Cancer Res 2002;62(3):917–923. [PubMed: 11830552]

48. Achbarou A, Kaiser S, Tremblay G, Ste-Marie LG, Brodt P, Goltzman D, Rabbani SA. Urokinase overproduction results in increased skeletal metastasis by prostate cancer cells in vivo. Cancer Res 1994;54(9):2372–2377. [PubMed: 8162583]

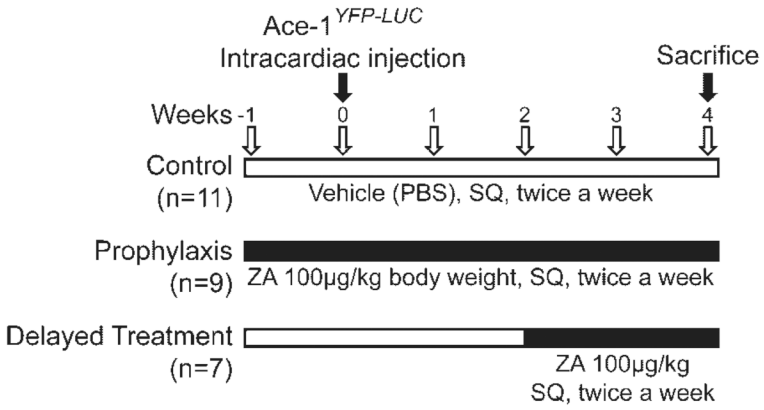

Fig. 1.

Treatment protocol. Nude mice were divided into three groups: the control group received PBS from –1 to 4 weeks (**top line**). The prophylaxis group received ZA from –1 to 4 weeks (**middle line**).The delayed treatment group received ZA from 2 to 4 weeks (**bottom line**). Mice were administered 100 µg/kg ZA BW, twice a week subcutaneously (SQ) to their respective groups. Ace-1$^{YFP-LUC}$ cells were injected on week 0.

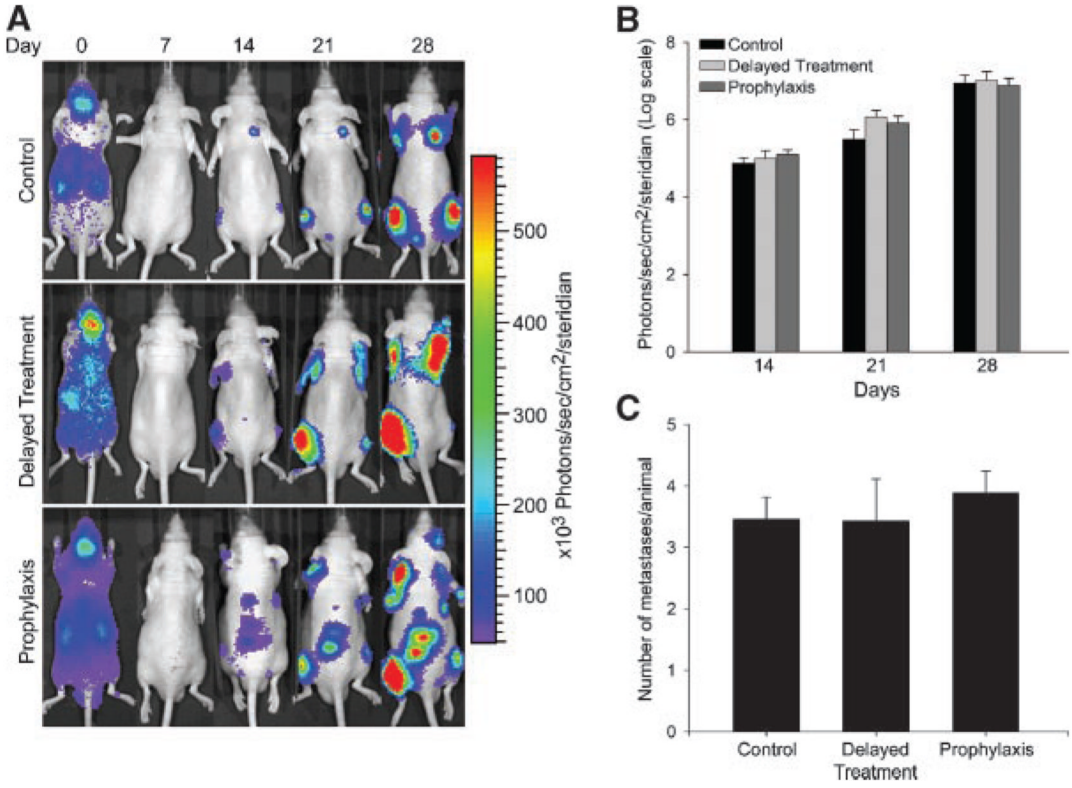

Fig. 2.

Effect of ZA on the Ace-1 tumor growth and metastasis incidence in nude mice was monitored using bioluminescence imaging (BLI). **A**: Representative images of serial BLI of Ace-1 tumor progression from control, delayed treatment and prophylaxis groups taken at 0,7,14,21, and 28 days, after intracardiac injection of cancer cells. On day 0, immediately after intracardiac injections, ACE-1 cells were present throughout the entire body and accumulated in the kidney, liver and brain. On day 7, BLI signals were gone. BLI signals were detected on day 14 at various sites of bone metastasis. At day 21 and 28, the intensity of BLI signals increased, which demonstrated progressive growth of the metastases. BLI on days 21 and 28 did not reveal any new metastatic sites compared to day14. **Panel B** graph represents the average intensity of the BLI signal measured at each metastatic region of interest (ROI) per group at the specific time points. Intensity of BLI was measured using Living Image software Version 2.50. **Panel C** graph shows the average number of metastases per group. Each region of interest was counted as one metastatic site.

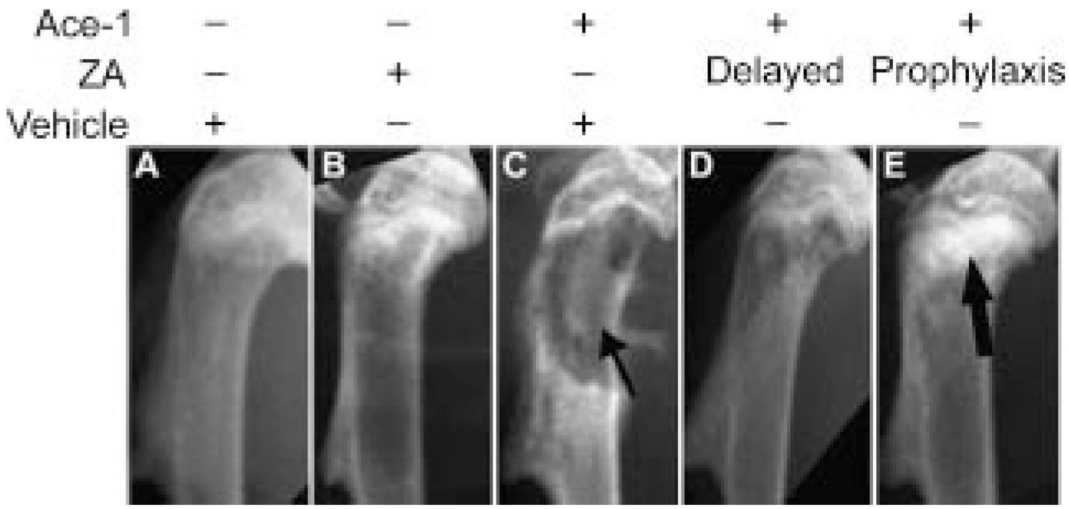

Fig. 3.

Radiographic evaluation of ZA on Ace-1 metastases to long bones. Radiographs of mice were taken 28 days after injection of Ace-1 tumor cells into the left cardiac ventricle. Cortical and trabecular bone lysis (thin arrows) was observed in the metaphyseal regions of long bones of mice that received Ace-1 cancer cells and vehicle (**C**) compared to mice that received vehicle alone (**A**). ZA-treated nontumor-bearing mice (**B**) had a mild increase in radioopacity in the proximal metaphysis of long bones compared to vehicle-treated nontumor-bearing mice (**A**). Mild trabecular bone loss and intact cortices were present in the delayed treatment group (**D**), whereas in the prophylactic group (**E**), intact cortices and increased radio-opacity of bone (thick arrow) was present in the metaphyseal region.

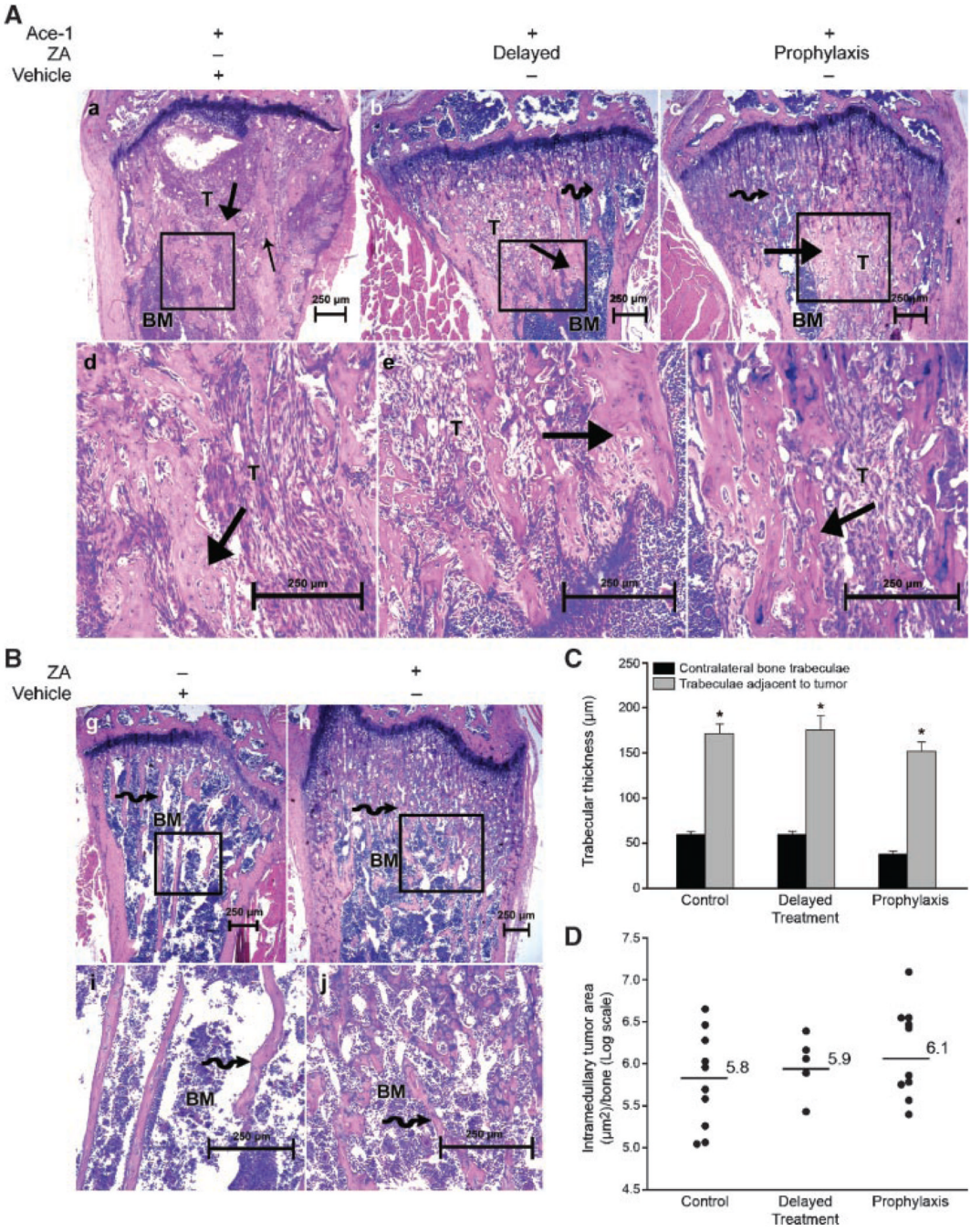

Fig. 4.

Histopathological evaluation of ZA on Ace-1 bone metastases. Mice were sacrificed 28 days after injection of Ace-1 cells into left cardiac ventricle. **Panel A, B**:H&E-stained sections of long bones. In all tumor-bearing mice (a–f), Ace-1 cells (T) replaced bone marrow (BM) cells in the metaphyseal region of the long bones. In tumor-bearing mice that received vehicle (a, d), there was cortical and trabecular bone lysis (thin arrow) and new woven bone production (thick arrows) in the medullary cavity adjacent to the tumor. In prophylactic and delayed treatment groups (b, c, e, f), intact cortices and new woven bone formation (thick arrow) characterized by thickened trabeculae were present adjacent to Ace-1 cells in the metaphyseal region. Increased trabecular density (curved arrow) was present in tumor-bearing (b, c) and

nontumor-bearing (**h, j**) mice that received ZA compared to the mice that received vehicle alone (**g, i**). **Panel C**: histomorphometric analysis showed that trabecular thickness in long bones adjacent to metastases was significantly greater than contralateral bones without metastases. *$P < 0.001$ (*t*-test) and data represent the mean ± SEM. **Panel D** shows a vertical dot plot of the individual values of tumor area from each long bone that was quantified.

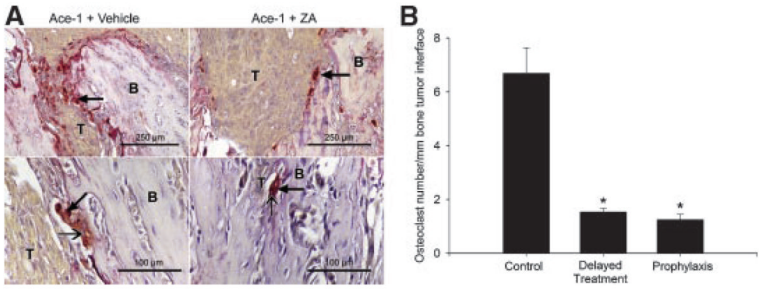

Fig. 5.

Effect of ZA on tartrate-resistant acid phosphatase (TRAP) activity of osteoclasts in Ace-1 tumor-bearing mice. TRAP-stained sections of bones demonstrated numerous red TRAP-positive osteoclasts (thick arrow) along the tumor (T)–bone (B) interface in Ace-1-bearing mice compared to few osteoclasts in ZA-treated mice (**A, top panels**).Higher magnification of TRAP-positive osteoclasts demonstrated multiple nuclei (thin head arrow) (A, **lower panels**). Histomorphometric analysis showed a significant decrease in TRAP-positive osteoclasts with three or more nuclei along the tumor-bone interface between control and ZA-treated groups (**Panel B**). *$P < 0.01$ (ANOVA and Dunn's test for posthoc analysis). Data represent the mean ± standard error of mean (SEM).

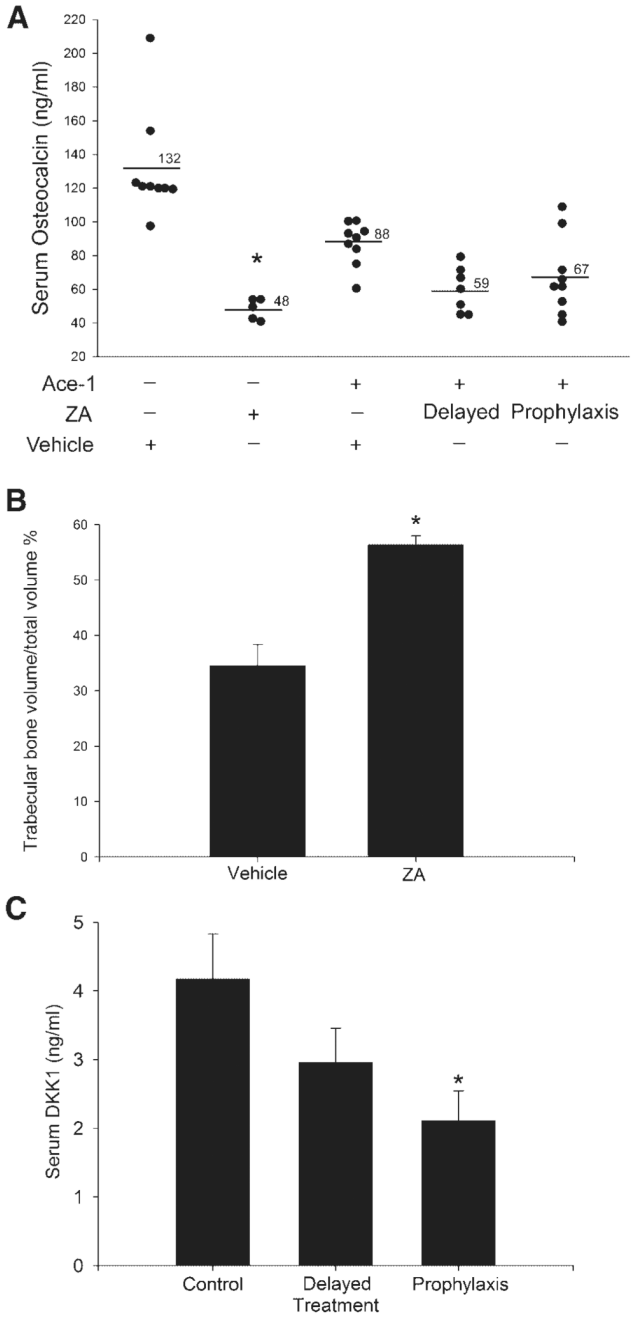

Fig. 6.

Effect of ZA on trabecular bone, Dkk1 and osteocalcin. In nontumor-bearing mice, ZA significantly decreased serum osteocalcin compared to mice that received vehicle alone. In tumor bearing mice, ZA had no significant effect on osteocalcin concentrations (**A**). **P* < 0.0001 compared to vehicle group. Histomorphometric analysis revealed that ZA significantly increased the trabecular bone volume in nontumor-bearing mice (**B**). **P* < 0.05 (*t*-test) and data represent the mean ± SEM. ZA decreased the serum Dkk1 concentrations in tumor-bearing mice in the prophylactic treatment group (**C**). **P* < 0.05 (Dunnett's simultaneous tests) compared to vehicle-treated tumor-bearing mice (control) and data represent mean ± SEM.